Published in final edited form as:
Circ Heart Fail. 2010 March ; 3(2): 306–313. doi:10.1161/CIRCHEARTFAILURE.109.864785.

Cardiac-specific overexpression of catalase identifies hydrogen peroxide-dependent and independent-phases of myocardial remodeling, and prevents the progression to overt heart failure in Gαq-overexpressing transgenic mice

Fuzhong Qin[1,2], **Shannon Lennon-Edwards**[1,2], **Steve Lancel**[1,2], **Andreia Biolo**[1,2], **Deborah A. Siwik**[1,2], **David R. Pimentel**[1,2], **Gerald W. Dorn**[3], **Y. James Kang**[4], and **Wilson S. Colucci**[1,2]

[1]Cardiovascular Medicine Section, Boston University Medical Center, Boston, MA

[2]Myocardial Biology Unit, Boston University Medical Center, Boston, MA

[3]Cardiovascular Medicine Section, University of Cincinnati, Cincinnati, Ohio

[4]Department of Toxicology, University of Louisville, Louisville, KY

Abstract

Background—While it appears that reactive oxygen species (ROS) contribute to chronic myocardial remodeling, questions remain about a) the specific type(s) of ROS involved, b) the role of ROS in mediating specific cellular events, and c) the cause and effect relationship between myocardial ROS and the progression to heart failure. Transgenic mice with myocyte-specific overexpression of Gαq develop a dilated cardiomyopathy that progresses to heart failure. We used this model to examine the role of H_2O_2 in mediating myocardial remodeling and the progression to failure.

Methods and Results—In Gαq myocardium, markers of oxidative stress were increased at 4 weeks and increased further at 20 weeks. Gαq mice were cross-bred with transgenic mice having myocyte-specific overexpression of catalase. At 4 weeks of age, left ventricular (LV) end-diastolic dimension (EDD) was increased and LV fractional shortening (FS) was decreased in Gαq mice, and deteriorated further through 20 weeks. In Gαq mice, myocardial catalase overexpression had no effect on LVEDD or FS at 4 weeks, but prevented the subsequent deterioration in both. In Gαq mice, myocyte hypertrophy, myocyte apoptosis and interstitial fibrosis were prevented by catalase overexpression, as was the progression to overt heart failure, as reflected by lung congestion and exercise intolerance.

Conclusion—In Gαq mice, myocyte-specific overexpression of catalase had no effect on the initial phenotype of LV dilation and contractile dysfunction, but prevented the subsequent progressive remodeling phase leading to heart failure. Catalase prevented the cellular hallmarks of

Correspondence: Wilson S. Colucci, M.D., Cardiovascular Medicine Section, Boston University Medical Center, 88 East Newton Street, Boston, MA 02118, Tel: 617-638 8706, Fax: 617-638 8712, wilson.colucci@bmc.org.

Disclosures

None.

adverse remodeling (myocyte hypertrophy, myocyte apoptosis and interstitial fibrosis) and the progression to overt heart failure. Thus, H_2O_2 and/or associated oxidant pathways play a critical role in adverse myocardial remodeling and the progression to failure.

Keywords

Free radicals; heart failure; remodeling; apoptosis; hypertrophy

Introduction

Several lines of evidence suggest that reactive oxygen species (ROS) contribute to adverse myocardial remodeling and the progression to failure (1;2). However, several important questions remain to be answered. First, relatively little is known about the specific type(s) of reactive oxygen species (ROS) involved (e.g., superoxide, hydrogen peroxide, peroxynitrite). Second, while ROS can cause several cellular events (e.g., myocyte hypertrophy, apoptosis, fibrosis) that participate in myocardial remodeling (1;3), little is known about the specific role of ROS in mediating these events. Finally, little is known about the cause and effect relationship of ROS to the overall progression to myocardial failure.

The G-protein, Gαq, mediates signaling for several stimuli (e.g., norepinephrine, angiotensin, mechanical strain) that cause hypertrophy and/or apoptosis in cardiac myocytes *in vitro* (4). The relevance of Gαq signaling for myocardial remodeling and failure *in vivo* (5) is supported by the demonstration that transgenic mice with cardiac myocyte-specific overexpression of Gαq develop myocardial remodeling which progresses to a dilated cardiomyopathy (6). Oxidative stress is increased in the myocardium of Gαq mice (7) and has been implicated in the pathophysiology of myocardial remodeling and failure in this model .

We therefore used Gαq mice to test the hypothesis that H_2O_2 mediates pathologic remodeling *in vivo* and to delineate the mechanisms involved. Accordingly, mice with cardiac-specific overexpression of Gαq were cross-bred with transgenic mice with myocyte-specific overexpression of catalase (8;9), the primary enzyme responsible for detoxification of H_2O_2. To understand the temporal relationship of myocardial H_2O_2 to the progression of myocardial remodeling, left ventricular (LV) dimensions and function were assessed serially from 4 to 20 weeks of age.

Methods

Experimental animals

Transgenic mice with cardiac-specific overexpression of Gαq (Gαq-40 mice, FVB/N) (6) and WT (FVB/N) mice were cross-bred with transgenic mice having myocyte-specific overexpression of catalase (Line 742; 60X catalase activity; FVB/N) (9). The resulting males (n=5-9 in each group) were used in this study. The protocol was approved by the Institutional Animal Care and Use Committee at Boston University School of Medicine.

Echocardiographic measurements

LV dimensions and function were measured in non-anesthetized mice using an Acuson Sequoia C-256 echocardiograph machine equipped with a 15 MHz linear transducer (model 15L8). Briefly, the heart was imaged in the 2-D parasternal short-axis view, and an M-mode echocardiogram of the mid-ventricle was recorded at the level of papillary muscles. Anterior wall thickness (AWT), posterior wall thickness (PWT), LV end-diastolic (EDD) and end-

systolic (ESD) dimensions were measured from the M-mode image. LV fractional shortening (FS) was calculated as (EDD–ESD) / EDD × 100. LV relative wall thickness (RWT) was calculated as (AWT+PWT) / EDD.

Exercise capacity

Maximal exercise capacity was tested at 20 weeks using a rodent treadmill with air puff motivation (10;11). Total exercise time was recorded as the elapsed time to exhaustion and then converted to distance. Exhaustion is defined as the point at which the animal can not keep pace with the treadmill (within 15 sec) despite the air flow motivator. The maximal exercise capacity was calculated as the total distance run by the animal during the exercise protocol.

Organ weight and histology

The mice were sacrificed at 20 weeks of age. Heart, LV with septum, lung and liver were weighed. LV samples were fixed in 10% buffered formalin, embedded with paraffin and then sectioned. Sections were stained with hematoxylin and eosin and examined under a light microscopy (BX 40, Olympus). Five random fields from each of 4 sections per animal were analyzed and 60 myocytes per animal were measured. The quantification of myocyte cross section area was determined using NIH ImageJ software. To assess fibrosis, sections were stained with Masson's trichrome kit (Sigma) and examined under a light microscope (BX 40, Olympus).

Immunohistochemistry for 3-nitrotyrosine and 4-hydroxy-2-nonenal

LV tissue sections (4 μm) were blocked with 10% goat serum in phosphate-buffered saline, incubated with rabbit anti-3-nitrotyrosine polyclonal antibody or mouse anti-HNE monoclonal antibody, and then incubated with goat biotin-conjugated anti-rabbit IgG or goat biotin-conjugated anti-mouse IgG (Vector Laboratory, Burlingame, CA). The sections were incubated with avidin and biotinylated horseradish peroxidase macromolecular complex (Vector Laboratory) and stained with 3-amino-9-ethylcarbazole (Vector Laboratory) and hematoxylin (Vector Laboratory). For negative control, the primary antibody was omitted instead of normal rabbit IgG or normal mouse IgG. The samples were examined under a light microscopy (BX 40, Olympus). Ten color images of 3-nitrotyrosine or 4-hydroxy-2-nonenal staining were randomly selected from four sections of the heart and photographed at a magnification of X40. The area and intensity of staining were blinded to score for quantification. The scoring range was the following: 0, no visible staining; 1, faint staining; 2 moderate staining; and 3, strong staining.

GSH/GSSG

The ratio of reduced to oxidized glutathione was determined in LV tissue homogenate as described using an Oxis GSH/GSSG-412 kit (12).

TUNEL staining

Apoptosis was assessed using an In Situ Cell Death Detection Fluorescein Kit (Roche Applied Science, Indianapolis, IN) according to the manufacturer's instructions. Briefly, LV sections were incubated with the reaction mixture containing terminal deoxynucleotidyl transferase and fluorescein-labeled dUTP. To identify cardiomyocytes, sections were incubated with mouse anti-α-sarcomeric actin monoclonal antibody (Sigma-Aldrich, St. Louis, MO) and then incubated with goat anti-mouse IgG conjugated TRITC (Sigma). Finally, to identify all nuclei (non-apoptotic and apoptotic), sections were stained with Hoechst 33258. The samples were analyzed under a fluorescence microscope (Diaphot 300, Nikon). Four sections per animal were analyzed. Cardiomyocyte nuclei were determined by

random counting of 10 fields per section. The number of apoptotic nuclei was calculated per 10,000 cardiomyocytes.

Statistical analysis

Results are presented as mean ± SEM. The statistical significance of differences among groups or between two means was determined using repeated measures analysis of variance and the Bonferroni test for multiple comparisons. The incidence of pleural effusions was tested by the Fisher exact test. $P>0.05$ was considered statistically significant.

Results

Age-related oxidative stress in the Gαq mouse heart

The ratio of reduced to oxidized glutathione, an index of overall cellular oxidative stress, was measured in hearts from WT and Gαq mice at 4 and 20 weeks of age. GSH was unchanged in Gαq vs. WT hearts at either age. In Gαq mice, GSSG was increased at 4 weeks and increased further at 20 weeks, and likewise, the GSH/GSSG ratio was decreased at 4 weeks and decreased further at 20 weeks (Figure 1). Consistent with the observed decrease in GSH/GSSG ratio at 20 weeks, immunohistochemical staining of myocardium from Gαq mice at this age demonstrated marked increases in two markers of oxidative stress, 3-nitrotyrosine and 4-hydroxy-2-nonenal, both of which were visualized diffusely over myocytes (Figure 2).

Catalase overexpression attenuates myocardial oxidative stress

Based on the observed increase in oxidative stress in the Gαq mouse heart, we cross-bred Gαq mice with mice that overexpress catalase in a myocyte-specific manner that were generated by Kang and colleagues (8;9). In the Gαq / catalase mice the intensities of both NY and HNE staining were reduced to the levels present in WT mice (Figure 2), and likewise, the GSH/GSSG ratio was normalized to a value similar to that in WT mice (Figure 2E). Thus, oxidative stress in the Gαq mouse heart is sensitive to myocyte-specific expression of catalase.

Time course of cardiac remodeling and failure

While several studies have demonstrated the development of severe dilated cardiomyopathy in Gαq mice, relatively little is known about the time course of remodeling (13;14). Accordingly, we performed echocardiography every 4 weeks beginning at 4 weeks of age, the first age at which these studies were feasible. At 4 weeks of age there was already marked eccentric LV remodeling with chamber dilation, reduced wall thickness and decreased fractional shortening (Figure 3). Subsequently, LV size and function remained relatively stable until 8 weeks of age, after which all progressively deteriorated (Figure 3).

Myocyte-specific catalase overexpression prevents the progressive remodeling phase

Myocyte-specific overexpression of catalase had no effect on any measure of remodeling at 4 or 8 weeks of age (Figure 3). However, beginning at 12 weeks of age catalase-overexpressing Gαq mice had significant improvements in all measures of remodeling, such that progression between 4 and 20 weeks of age was almost completely halted. Thus, while the early phenotype in this genetic model is not catalase-sensitive, the subsequent progressive phenotype is highly sensitive to catalase.

Myocyte-specific catalase overexpression prevents myocyte hypertrophy, apoptosis and interstitial fibrosis

At 20 weeks, LV weight in Gαq mice was increased ≈14%. The increase in LV weight was prevented in the Gαq / catalase mice (Table 1). Likewise, myocyte cross-sectional area was markedly increased in Gαq mice (vs. WT) and the increase was attenuated, but not completely prevented in Gαq / catalase mice (Figure 4). Myocardial fibrosis, assessed by Masson's trichrome staining, revealed increased interstitial fibrosis in Gαq mice that was almost completely prevented in Gαq / catalase mice (Figure 5).

Myocyte apoptosis was assessed by TUNEL staining using triple labeling to co-localize fragmented nuclear DNA, nuclei (Hoechst 33342) and α-sarcomeric actin. Specificity of the technique to detect DNA fragmentation was documented by positive labeling of nuclei after exposure to DNase I (Figure 6, **Panels A – D**). DNA fragmentation was absent when the terminal deoxynucleotidyl transferase was omitted in the enzymatic reaction (data not shown). Representative images from WT, Gαq and Gαq / catalase mice are shown in Figure 6 **(Panels E-P)**. Quantification of apoptotic myocytes demonstrated an approximately 9-fold increase in Gαq mice that was almost completely prevented in Gαq / catalase mice (Figure 6, **Panel Q**).

Catalase prevents the development of overt heart failure

Gαq mice had evidence of functional impairment with an approximately 40% reduction in maximal exercise capacity, as compared to WT mice. In Gαq / catalase mice exercise capacity was preserved and similar to that in WT mice (Figure 7). Over the course of 20 weeks, one Gαq mouse died, while no WT, catalase or Gαq/catalase mice died. Of the surviving Gαq mice, 80% had pleural effusions at sacrifice, whereas pleural effusion was not evident in any WT, catalase or Gαq/catalase mice (Table 1). Likewise, at sacrifice lung weight was increased in the Gαq mice, indicative of lung congestion, and the increase was prevented by catalase overexpression (Table 1). Thus, at 20 weeks of age in the Gαq mice there was functional and anatomical evidence of overt heart failure which was prevented by myocyte-specific expression of catalase.

Discussion

The major new finding of this study is that myocyte-specific expression of catalase has no effect on the initial abnormal myocardial phenotype in Gαq mice, but largely prevents subsequent progressive LV remodeling and the development of overt heart failure. The beneficial effect of catalase is associated with marked inhibition of myocyte hypertrophy, myocyte apoptosis and interstitial fibrosis. These findings address several fundamental, unresolved questions about the role of ROS in myocardial failure.

Mice with myocyte-specific expression of Gαq develop a severe dilated cardiomyopathy (6;13-15). Since most studies in the Gαq mouse have focused on a single time point, relatively little is known about the time course over which myocardial remodeling and progression to heart failure occur. Echocardiography at 4 weeks of age, immediately after weaning, showed marked LV dilation, eccentric hypertrophy and systolic dysfunction. We can not determine the time course of this early phase of adverse remodeling. Between 4 and 8 weeks of age there was only slight worsening in LV structure and function, but by 12 weeks there was clear deterioration with further LV dilation and systolic dysfunction that steadily worsened through 20 weeks of age. Thus, in the Gαq mice there was an initial phase (4 weeks) marked by myocardial dysfunction that was followed by a second phase (12 – 20 weeks) characterized by progressive remodeling and failure.

Increased oxidative stress in the myocardium has been observed in several animal models of heart failure including pressure overload (16;17), myocardial infarction (18) and rapid pacing (19), and in humans with heart failure (20). In the Gαq mouse we found that immunohistochemical staining for two markers of oxidative stress, 3-nitrotyrosine and 4-hydroxy-2-nonenal, was positive at 20 weeks of age. Likewise, at 20 weeks the ratio of reduced-to-oxidized glutathione (GSH/GSSG), a measure of overall cellular oxidative stress, was markedly reduced due to an increase in GSSG. Of note, the GSH/GSSG ratio was also decreased at 4 weeks of age, the earliest age studied, but was less reduced than at 20 weeks, indicating that myocardial oxidative stress in the Gαq mouse heart increases over time. These findings are consistent with those of Satoh et al. (7), who recently showed increased levels of ROS and peroxide-derived oxygen radicals in the Gαq mouse heart at 14 – 15 weeks of age. Our study thus confirms the presence of increased myocardial oxidative stress in this and other heart failure models, and further, demonstrates that oxidative stress increases with the progression of LV remodeling.

To assess the relationship between increased oxidative stress and myocardial remodeling in the Gαq mouse heart, we cross-bred Gαq mice with mice that have myocyte-specific expression of catalase. The catalase mouse overexpresses catalase by ≈ 60-fold, and has been shown to rescue the cardiac effects of doxorubicin (9) and ischemia/reperfusion (8). The concurrent overexpression of catalase in Gαq mice had no effect on the initial phenotype, as assessed by echocardiography. In striking contrast, catalase abolished the subsequent progressive deterioration that occurred after 8 weeks such that there were no further changes in LV diameter, wall thickness or systolic function. In parallel, catalase restored the protein markers of oxidative stress, NY and HNE, to control levels observed in normal mice. One limitation of our study is that we do not know the exact time at which catalase expression increased. However, both the catalase and Gαq transgenes are under the control of the α-myosin heavy chain promoter (21), and therefore the expression of both would be expected to increase rapidly in the days immediately after birth.

In cardiac myocytes *in vitro*, we (22-24) and others (25) have shown that ROS, including H_2O_2, can cause hypertrophy and apoptosis, hallmarks of myocardial remodeling (1-3). An important feature of the dilated cardiomyopathy in the Gαq mouse is eccentric hypertrophy with severe LV wall thinning relative to chamber diameter. At the cellular level this cardiomyopathy is associated with myocyte hypertrophy and apoptosis, both of which were essentially abolished by catalase, as was progressive wall thinning. Thus, these data clearly indicate that myocyte hypertrophy and apoptosis that occur during the progression phase are sensitive to catalase, and thus, mediated by ROS. It should be noted that myocyte widening, as observed in this study, is more typical of concentric hypertrophy but also may occur in eccentric hypertrophy in conjunction with myocyte lengthening. In addition, given the marked decrease in wall thickness observed by echocardiography, the finding of myocyte widening suggests that there is myocyte loss, as would be expected based on the increased rate of apoptosis observed.

Recently, Satoh et al. (7) showed in the Gαq mouse that estrogen markedly improve remodeling in association with decreased levels of ROS, increased expression of the thioredoxin system, and inhibition of apoptosis-related signaling kinasse-1 (ASK). They concluded that estrogen ameliorated heart failure by antioxidant mechanisms that involve the upregulation of thioredoxin and inhibition of Rac1-mediated nicotinamide adenine dinucleotide phosphate oxidase activity and apoptosis signal-regulating kinase-1. Our observations support the importance of oxidative stress in this model, and provide further information about the specific role of H_2O_2 and/or associated oxidative pathways in mediating myocyte apoptosis, myocyte hypertrophy and fibrosis.

Oxidative stress is systemic in heart failure (26-28) and may be involved in wide-ranging effects on the vasculature and other organs that can influence cardiac remodeling. Prior studies that have examined the role of ROS in myocardial remodeling have employed the systemic administration of antioxidants such as probucol (29), EUK-8 (30), dimethylthiourea (31), vitamins A and/or E (32), estrogen (7) or the generalized overexpression of an antioxidant enzyme (33). Thus, an important and unique feature of the myocyte-specific Gαq and catalase mice used in this study is that the resulting observations allow conclusions about the role of ROS in the myocyte, per se. In this regard, it is interesting that myocyte-specific catalase expression markedly suppressed interstitial fibrosis in the Gαq mouse. This suggests that H_2O_2 in the myocyte mediates fibrosis, perhaps directly via the elaboration of collagen regulatory proteins (34) and / or indirectly via paracrine effects on neighboring fibroblasts (35).

Although superoxide anion is the primary type of ROS generated by mitochondria and oxidases in the heart, it is both short-lived due to rapid dismutation to H_2O_2 by superoxide dismutases and membrane impermeant. By contrast, H_2O_2 is relatively longer-lived and membrane permeant. H_2O_2 itself is reactive and may generate highly reactive hydroxyl radicals. Superoxide, H_2O_2 and hydroxyl radicals have all been observed to be increased in failing myocardium (19;36). While our data are consistent with a direct role for H_2O_2 in mediating the observed events, it is also possible that some or all of these events are mediated by other ROS species that are up- or down-stream of H_2O_2.

In the Gαq mouse, the effects of catalase distinguish the initial phenotype from the progressive remodeling that eventually results in overt heart failure, and in so doing, suggest that in this model these phases involve distinct pathophysiologies. The initial phenotype in the Gαq mouse may be a reflection of transcriptionally-determined events mediated by Gαq. A consequence of this initial phenotype is the stimulation of a subsequent, ROS-dependent remodeling process. It is noteworthy that catalase prevented the progression of myocardial remodeling and the subsequent development of overt failure with lung congestion, pleural effusions and exercise intolerance. In patients the development of clinical heart failure is often the culmination of months or years of remodeling following a discrete injury to the myocardium (e.g., myocardial infarction). With time, progressive myocardial remodeling leads to declining cardiovascular function and overt heart failure. In this regard it is of interest that in the Gαq mouse the early phenotype, while associated with substantial abnormalities in LV geometry and function, was not associated with a reduction in exercise capacity. This finding might be analogous to the clinical setting in a patient with asymptomatic LV dysfunction. These observations thus raise the possibility that strategies to inhibit the ROS-dependent phase of myocardial remodeling may be of value in the prevention of heart failure in humans.

Acknowledgments

Sources of Funding

This work was supported by NIH grants HL61639 and HL20612 (W.S.C), a grant from La Fondation pour la Recherche Médicale SPE20051105207 (S.L.), and a CAPES-BR fellowship (A.B.).

References

1. Sawyer DB, Siwik DA, Xiao L, et al. Role of oxidative stress in myocardial hypertrophy and failure. J Mol Cell Cardiol. 2002; 34:379–388. [PubMed: 11991728]
2. Seddon M, Looi YH, Shah AM. Oxidative stress and redox signalling in cardiac hypertrophy and heart failure. Heart. 2007; 93:903–907. [PubMed: 16670100]

3. Mann DL, Bristow MR. Mechanisms and models in heart failure: the biomechanical model and beyond. Circulation. 2005; 111:2837–2849. [PubMed: 15927992]
4. Dorn GW, Brown JH. Gq signaling in cardiac adaptation and maladaptation. Trends Cardiovasc Med. 1999; 9:26–34. [PubMed: 10189964]
5. Samarel AM. Gq-coupled receptor signaling in pathological ventricular remodeling. J Mol Cell Cardiol. 2001; 33:1399–1403. [PubMed: 11448129]
6. D'Angelo DD, Sakata Y, Lorenz JN, et al. Transgenic Galphaq overexpression induces cardiac contractile failure in mice. Proc Natl Acad Sci U S A. 1997; 94(15):8121–8126. [PubMed: 9223325]
7. Satoh M, Matter CM, Ogita H, et al. Inhibition of apoptosis-regulated signaling kinase-1 and prevention of congestive heart failure by estrogen. Circulation. 2007; 115:3197–3204. [PubMed: 17562954]
8. Li G, Chen Y, Saari JT, et al. Catalase-overexpressing transgenic mouse heart is resistant to ischemia-reperfusion injury. Am J Physiol. 1997; 273:H1090–5. [PubMed: 9321793]
9. Kang YJ, Chen Y, Epstein PN. Suppression of doxorubicin cardiotoxicity by overexpression of catalase in the heart of transgenic mice. J Biol Chem. 1996; 271:12610–12616. [PubMed: 8647872]
10. Biolo A, Greferath R, Siwik DA, et al. Enhanced exercise capacity in mice with severe heart failure treated with an allosteric effector of hemoglobin, myo-inositol trispyrophosphate. Proc Natl Acad Sci U S A. 2009; 106:1926–1929. [PubMed: 19204295]
11. Trueblood NA, Inscore PR, Brenner D, et al. Biphasic temporal pattern in exercise capacity after myocardial infarction in the rat: relationship to left ventricular remodeling. Am J Physiol Heart Circ Physiol. 2005; 288:H244–H249. [PubMed: 15358607]
12. Ago T, Sadoshima J. Thioredoxin and ventricular remodeling. J Mol Cell Cardiol. 2006; 41:762–773. [PubMed: 17007870]
13. Sakata Y, Hoit BD, Liggett SB, et al. Decompensation of pressure-overload hypertrophy in G alpha q-overexpressing mice. Circulation. 1998; 97:1488–1495. [PubMed: 9576430]
14. Hayakawa Y, Chandra M, Miao W, et al. Inhibition of cardiac myocyte apoptosis improves cardiac function and abolishes mortality in the peripartum cardiomyopathy of Galpha(q) transgenic mice. Circulation. 2003; 108:3036–3041. [PubMed: 14638549]
15. Adams JW, Sakata Y, Davis MG, et al. Enhanced Galphaq signaling: a common pathway mediates cardiac hypertrophy and apoptotic heart failure. Proc Natl Acad Sci U S A. 1998; 95:10140–10145. [PubMed: 9707614]
16. Kuster GM, Kotlyar E, Rude MK, et al. Mineralocorticoid receptor inhibition ameliorates the transition to myocardial failure and decreases oxidative stress and inflammation in mice with chronic pressure overload. Circulation. 2005; 111:420–427. [PubMed: 15687129]
17. Maytin M, Siwik DA, Ito M, et al. Pressure overload-induced myocardial hypertrophy in mice does not require gp91phox. Circulation. 2004; 109:1168–1171. [PubMed: 14981002]
18. Liu YH, Carretero OA, Cingolani OH, et al. Role of inducible nitric oxide synthase in cardiac function and remodeling in mice with heart failure due to myocardial infarction. Am J Physiol Heart Circ Physiol. 2005; 289:H2616–H2623. [PubMed: 16055518]
19. Ide T, Tsutsui H, Kinugawa S, et al. Direct evidence for increased hydroxyl radicals originating from superoxide in the failing myocardium. Circ Res. 2000; 86:152–157. see comments. [PubMed: 10666410]
20. Nakamura K, Kusano K, Nakamura Y, et al. Carvedilol decreases elevated oxidative stress in human failing myocardium. Circulation. 2002; 105:2867–2871. [PubMed: 12070115]
21. Subramaniam A, Jones WK, Gulick J, et al. Tissue-specific regulation of the alpha-myosin heavy chain gene promoter in transgenic mice. J Biol Chem. 1991; 266:24613–24620. [PubMed: 1722208]
22. Kwon SH, Pimentel DR, Remondino A, et al. H(2)O(2) regulates cardiac myocyte phenotype via concentration-dependent activation of distinct kinase pathways. J Mol Cell Cardiol. 2003; 35:615–621. [PubMed: 12788379]
23. Xiao L, Pimentel DR, Wang J, et al. Role of reactive oxygen species and NAD(P)H oxidase in alpha(1)- adrenoceptor signaling in adult rat cardiac myocytes. Am J Physiol Cell Physiol. 2002; 282:C926–C934. [PubMed: 11880281]

24. Remondino A, Kwon SH, Communal C, et al. Beta-adrenergic receptor-stimulated apoptosis in cardiac myocytes is mediated by reactive oxygen species/c-Jun NH2-terminal kinase-dependent activation of the mitochondrial pathway. Circ Res. 2003; 92:136–138. [PubMed: 12574140]
25. Sabri A, Hughie HH, Lucchesi PA. Regulation of hypertrophic and apoptotic signaling pathways by reactive oxygen species in cardiac myocytes. Antioxid Redox Signal. 2003; 5:731–740. [PubMed: 14588146]
26. Keith M, Geranmayegan A, Sole MJ, et al. Increased oxidative stress in patients with congestive heart failure. J Am Coll Cardiol. 1998; 31:1352–1356. [PubMed: 9581732]
27. Braunwald E. Biomarkers in heart failure. N Engl J Med. 2008; 358:2148–2159. [PubMed: 18480207]
28. Radovanovic S, Krotin M, Simic DV, et al. Markers of oxidative damage in chronic heart failure: role in disease progression. Redox Rep. 2008; 13:109–116. [PubMed: 18544228]
29. Nakamura R, Egashira K, Machida Y, et al. Probucol attenuates left ventricular dysfunction and remodeling in tachycardia-induced heart failure: roles of oxidative stress and inflammation. Circulation. 2002; 106:362–367. [PubMed: 12119254]
30. van Empel VP, Bertrand AT, van Oort RJ, et al. EUK-8, a superoxide dismutase and catalase mimetic, reduces cardiac oxidative stress and ameliorates pressure overload-induced heart failure in the harlequin mouse mutant. J Am Coll Cardiol. 2006; 48:824–832. [PubMed: 16904556]
31. Kinugawa S, Tsutsui H, Hayashidani S, et al. Treatment with dimethylthiourea prevents left ventricular remodeling and failure after experimental myocardial infarction in mice: role of oxidative stress. Circ Res. 2000; 87:392–398. [PubMed: 10969037]
32. Dhalla AK, Hill MF, Singal PK. Role of oxidative stress in transition of hypertrophy to heart failure. J Am Coll Cardiol. 1996; 28(2):506–514. [PubMed: 8800132]
33. Shiomi T, Tsutsui H, Matsusaka H, et al. Overexpression of glutathione peroxidase prevents left ventricular remodeling and failure after myocardial infarction in mice. Circulation. 2004; 109:544–549. [PubMed: 14744974]
34. Siwik DA, Pagano PJ, Colucci WS. Oxidative stress regulates collagen synthesis and matrix metalloproteinase activity in cardiac fibroblasts. Am J Physiol Cell Physiol. 2001; 280:C53–C60. [PubMed: 11121376]
35. Siwik DA, Chang DL, Colucci WS. Interleukin-1beta and Tumor Necrosis Factor-alpha Decrease Collagen Synthesis and Increase Matrix Metalloproteinase Activity in Cardiac Fibroblasts In Vitro. Circ Res. 2000; 86:1259–1265. [PubMed: 10864917]
36. Ide T, Tsutsui H, Kinugawa S, et al. Mitochondrial electron transport complex I is a potential source of oxygen free radicals in the failing myocardium. Circ Res. 1999; 85:357–363. [PubMed: 10455064]

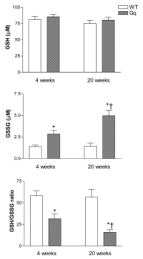

Figure 1.

Concentrations of reduced glutathione (GSH), oxidized glutathione (GSSG) and the ratio of reduced to oxidized glutathione (GSH/GSSG) in left ventricular myocardium of wild-type (WT) and Gαq mice at 4 and 20 weeks. Values are means ± SEM; n=5-6. *P>0.02 vs. WT. †P>0.05 vs. 4-week Gαq.

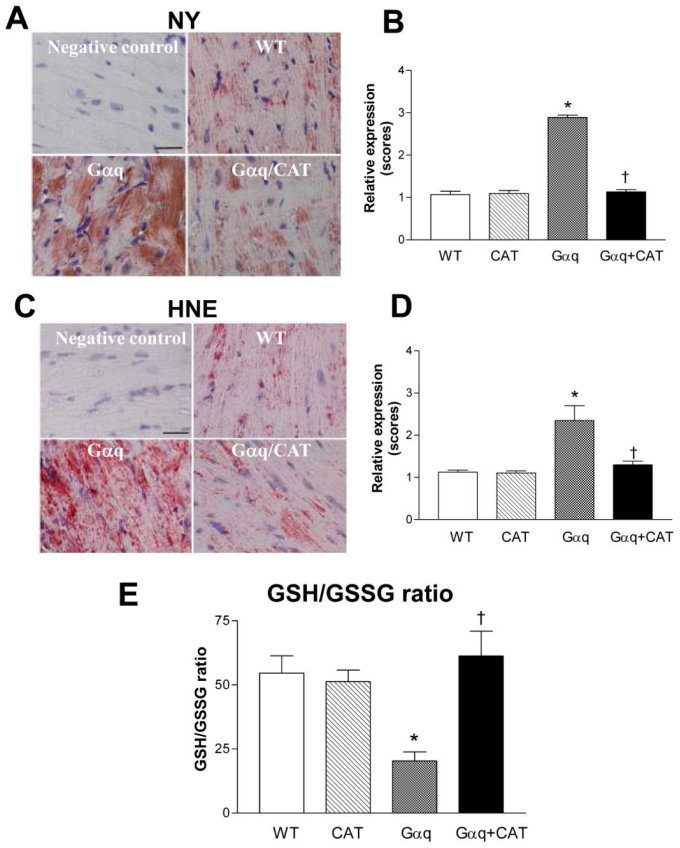

Figure 2.

Panels A-D depict immunohistochemical staining for 3-nitrotyrosine (NY) and 4-hydroxy-2-nonenal (HNE) in left ventricular myocardium of wild-type (WT), catalase (CAT), Gαq and Gαq/CAT mice at 20 weeks. In Gαq mice (vs. WT), myocardial NY and HNE expression were increased, and the increases in both were prevented in Gαq/CAT mice. NY or HNE staining is shown in red. Nuclei are shown in blue. The bar graphs show the relative expression of myocardial NY or HNE in the four groups. Values are means ± SEM; n=5-6. *P>0.001 vs. WT. †P>0.001 vs. Gαq. The bar in the negative control panels indicates 25 μm. . **Panel E** shows the ratio of reduced to oxidized glutathione (GSH/GSSG) in left ventricular myocardium of WT, CAT, Gαq and Gαq/CAT mice at 20 weeks. In Gαq mice (vs. WT), the ratio of GSH/GSSG was decreased, and the decrease was prevented in Gαq/CAT mice. Values are means ± SEM; n=5. *P>0.002 vs. WT. †P>0.005 vs. Gαq.

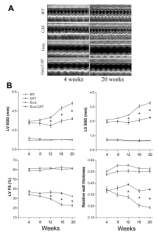

Figure 3.

Panel A depicts representative M-mode echocardiograms in wild-type (WT), catalase (CAT), Gαq and Gαq / CAT mice at 4 and 20 weeks of age. **Panel B** depicts the mean changes in left ventricular (LV) end-diastolic (EDD) and end-systolic (ESD) dimensions, LV fractional shortening (FS) and the relative wall thickness (RWT) in wild-type (WT), catalase (CAT), Gαq and Gαq / CAT mice at 4, 8, 12, 16 and 20 weeks of age. In Gαq mice (vs. WT), LV dilatation, relative wall thinning and contractile dysfunction were present at 4 weeks and progressively worsened between 12 and 20 weeks. Myocardial catalase (CAT) overexpression in Gαq mice had no effect on LV dilatation, wall thinning or contractile dysfunction at 4 weeks, but prevented deterioration in all three aspects of the phenotype between 12 and 20 weeks. RWT = (interventricular septal + posterior wall thickness at diastole) / LV EDD. Values are means ± SEM; n=5-9. *P>0.005 vs. Gαq group.

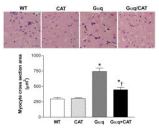

Figure 4.

Changes in myocyte cross sectional area in left ventricular myocardium of wild-type (WT), catalase (CAT), Gαq and Gαq/CAT mice at 20 weeks of age. The upper panels show representative photomicrographs of left ventricular tissue stained by hematoxylin and eosin. The lower panel shows mean myocyte cross sectional area as measured by NIH ImageJ. In Gαq mice (vs. WT), myocyte cross sectional area was increased, and the increase was reduced in Gαq/CAT mice. Values are means ± SEM; n=4-5. *P>0.02 vs. WT group. †P>0.05 vs. Gαq group. The bar in the left upper panel indicates 25 μm.

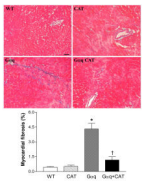

Figure 5.

Representative photomicrographs of Masson Trichrome staining for fibrosis in left ventricular myocardium of wild-type (WT), catalase (CAT), Gαq and Gαq/CAT mice at 20 weeks lf age. Increased myocardial fibrosis was present in Gαq mice, and was inhibited in Gαq/CAT mice. Myocardium stains red, and collagen stains blue. The bar in the left upper panel indicates 50 μm.

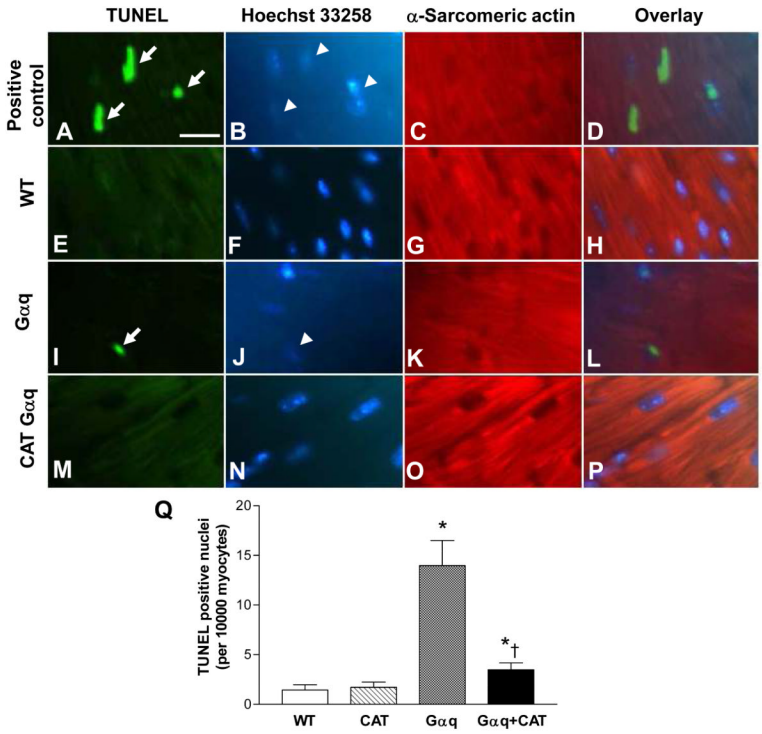

Figure 6.

Panels A-P depict representative photomicrographs of left ventricular tissue showing TUNEL staining for apoptotic myocytes. Apoptotic nuclei (arrows) are shown by green fluorescence in Panels A, E, I and M. Nuclei (arrowheads) stained by Hoechst 33258 are shown blue in Panels B, F, J and N. Cardiomyocytes identified by α-sarcomeric actin staining are shown red in Panels C, G, K and O. The overlays in Panels D, H, L and P allow identification of apoptotic nuclei present in myocytes. The bar in Panel A indicates 25 μm. **Panel Q** shows the mean group data. Changes in the number of apoptotic myocytes in left ventricular myocardium of wild-type (WT), catalase (CAT), Gαq and Gαq/CAT mice at 20 weeks. In Gαq (vs. WT) mice, myocyte apoptosis was increased, and the increase was reduced in Gαq/CAT mice. Values are means ± SEM; n=5-6. *P>0.005 vs. WT group. †P>0.005 vs. Gαq group.

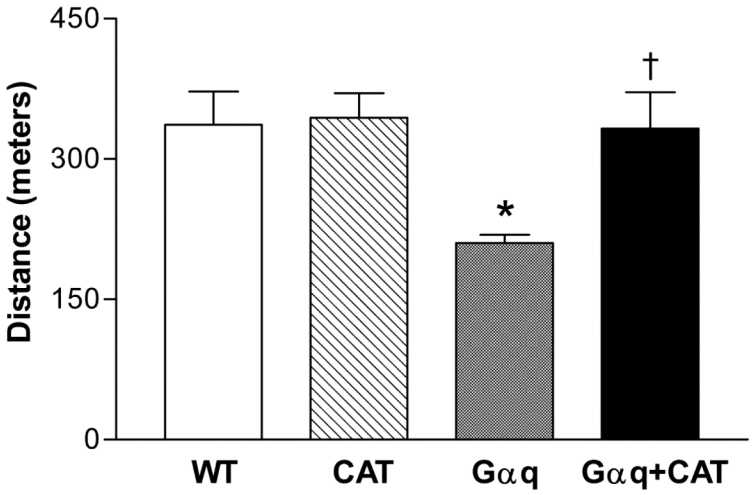

Figure 7.

Changes in maximal exercise capacity in wild-type (WT), catalase (CAT), Gαq and Gαq/CAT mice at 20 weeks. At 20 weeks, maximal exercise capacity was decreased in Gαq mice (vs. WT), but was preserved in Gαq/CAT mice. Values are means ± SEM; n=5-9. *P>0.05 vs. WT group. †P>0.05 vs. Gαq group.

Table 1

Body and organ weights

	WT	CAT	Gαq	Gαq / CAT
n	6	9	5	5
BW (g)	31.7 ± 1.4	30.9 ± 0.8	34.1 ± 1.0	32.3 ± 0.9
HW (mg)	138.0 ± 3.1	142.6 ± 3.8	189.6 ± 7.1*	161.7 ± 7.5*†
HW / BW (mg/g)	4.39 ± 0.14	4.63 ± 0.09	5.57 ± 0.18*	4.99 ± 0.16*†
LV W (mg)	95.9 ± 2.6	96.8 ± 2.5	109.5 ± 2.7*	98.3 ± 3.1†
LV W / BW (mg/g)	3.04 ± 0.06	3.08 ± 0.04	3.21 ± 0.02*	3.04 ± 0.03†
Lung W (mg)	166.1 ± 8.2	170.9 ± 5.0	211.5 ± 8.4*	179.5 ± 4.5*
Lung W / BW (mg/g)	5.25 ± 0.15	5.55 ± 0.16	6.22 ± 0.26*	5.56 ± 0.12†
Lung W (wet/dry)	4.29 ± 0.12	4.40 ± 0.06	4.76 ± 0.14*	4.18 ± 0.20†
Liver W (g)	1.37 ± 0.05	1.33 ± 0.03	1.47 ± 0.03	1.36 ± 0.03
Liver W / BW (g/g)	0.043 ± 0.001	0.043 ± 0.001	0.043 ± 0.002	0.042 ± 0.001
Pleural effusion	0/6	0/9	4/5*	0/5†

BW: body weight; HW: heart weight; LV: left ventricular. W: weight; WT: wild-type. CAT: catalase. Values are mean ± SE.

*P<0.05 vs. WT group.

†P<0.05 vs. Gαq group.